catalysts

MDPI

Article

Synergistic Effects of Photocatalysis, Ozone Treatment, and Metal Catalysts on the Decomposition of Acetaldehyde

Tsuyoshi Ochiai [1,*], Kengo Hamada [1] and Michifumi Okui [2]

[1] Kawasaki Technical Support Department, Local Independent Administrative Agency Kanagawa Institute of Industrial Science and Technology (KISTEC), Ground Floor East Wing, Innovation Center Building, KSP, 3-2-1 Sakado, Takatsu-ku, Kawasaki 213-0012, Japan; k-hamada@kistec.jp

[2] Manufacturing Innovation Division R&D Department, Fuji Industrial, Co., Ltd., 2-1-9 Fuchinobe, Chuo-ku, Sagamihara 252-0206, Japan; okui@fujioh.com

* Correspondence: pg-ochiai@kistec.jp

Abstract: This study explores the synergistic interactions between photocatalysis, ozone treatment, and metal catalysts in the decomposition of acetaldehyde, a representative volatile organic compound (VOC). The study addresses the growing need for efficient air purification technologies by integrating advanced oxidation processes. Metal catalysts, particularly manganese oxide-based materials, were combined with photocatalysis and ozonation to investigate their impact on acetaldehyde removal efficiency. Experimental results revealed that the treatment integrating these methods significantly outperformed conventional single-process treatments. Metal catalysts facilitated the initial oxidation of acetaldehyde, while photocatalysis accelerated subsequent stages, including the mineralisation of intermediates. Ozone contributed additional reactive oxidative species, further enhancing decomposition rates. These findings provide valuable insights into the design of efficient VOC removal systems, demonstrating that integrating metal catalysts with photocatalytic and ozonation processes offers a promising strategy for improving air purification technologies. This approach has potential applications in environmental remediation and indoor air quality management.

Keywords: photocatalysis; ozone; metal catalysts; air purification; acetaldehyde decomposition

Academic Editor: Hongxing Dai

Received: 29 December 2024
Revised: 24 January 2025
Accepted: 28 January 2025
Published: 3 February 2025

Citation: Ochiai, T.; Hamada, K.; Okui, M. Synergistic Effects of Photocatalysis, Ozone Treatment, and Metal Catalysts on the Decomposition of Acetaldehyde. *Catalysts* **2025**, *15*, 141. https://doi.org/10.3390/catal15020141

1. Introduction

Air quality management, particularly the removal of volatile organic compounds (VOCs), remains a critical environmental and public health challenge. Among the various VOCs, acetaldehyde has emerged as a significant concern due to its ubiquitous presence in indoor and outdoor environments and its well-documented health risks. This study examines an innovative approach to acetaldehyde decomposition by investigating the synergistic effects of three distinct technologies: photocatalysis, ozone treatment, and metal catalysts.

Photocatalysis is a highly promising technology for environmental remediation, particularly in air purification applications. Among various photocatalysts, titanium dioxide (TiO_2) is notable for its exceptional ability to generate and recombine charge carriers, a process critical for the oxidative degradation of organic pollutants [1–3]. The photocatalytic capabilities of TiO_2 have been extensively studied, with research highlighting its effectiveness in breaking down various organic compounds, including VOCs [4–7].

Ozone treatment is another highly effective method for VOC degradation, harnessing its strong oxidative properties. When combined with photocatalysis and metal catalysts, ozone has demonstrated remarkable potential for enhancing pollutant degradation rates [8–10]. This synergistic interaction has generated considerable interest in the development of more advanced air purification systems. Recent studies have demonstrated that integrating ozone with photocatalytic processes can significantly improve the efficiency of decomposing various VOCs, including complex aromatic compounds [11].

Metal catalysts are integral to this integrated approach. Systems utilising metals such as silver, copper, zinc, and, particularly, manganese have been extensively studied for their catalytic properties and ability to enhance photocatalytic performance [12,13]. Incorporating metal nanoparticles into photocatalytic systems has been shown to significantly boost pollutant degradation efficiency [3]. Manganese oxide-based materials have emerged as highly effective catalysts for low-temperature VOC elimination, offering energy-efficient solutions for air purification. Moreover, this approach effectively accomplishes two goals simultaneously: eliminating harmful ozone while utilizing it as an oxidant for VOC decomposition. Manganese oxide-based materials are particularly well-suited for this application due to their excellent ozone decomposition ability and oxidation properties. Recent progress in catalytic ozonation has revealed intricate mechanisms involving both the Langmuir–Hinshelwood and Mars–van Krevelen pathways. These findings illustrate how various metal catalysts interact with ozone and organic compounds [14]. Such interactions are highly dependent on the specific VOC type and operational conditions, necessitating the precise optimisation of system parameters to achieve maximum efficiency.

The integration of the three technologies—photocatalysis, ozone treatment, and metal catalysts—offers a promising solution to the limitations of single-method treatments. Previous studies have demonstrated that, while individual methods can be effective, they often encounter challenges such as incomplete degradation, the formation of unwanted by-products, or reduced efficiency under specific conditions [15]. Combining these processes can produce synergistic effects that enhance overall decomposition efficiency while potentially lowering energy consumption and operational costs.

This study aims to bridge a significant gap in the existing literature by providing an in-depth analysis of the combined effects of photocatalysis, ozone treatment, and metal catalysts on acetaldehyde decomposition. By integrating these methods, we propose an innovative and highly efficient approach to air purification, with the potential to significantly improve VOC removal across various environments. This research specifically focuses on elucidating the mechanisms of interaction among these processes and their collective impact on decomposition efficiency. We assessed the effectiveness of combining a photocatalytic filter and ozone gas introduction with an established metal-catalyst-based deodorising filter for VOC removal. Using two types of filters—each incorporating a photocatalyst and a metal catalyst—we aimed to achieve the efficient removal of relatively high concentrations of VOCs through the precise design and optimisation of treatment parameters. This approach not only addresses practical challenges in air purification but also advances the fundamental understanding of complex catalytic interactions in environmental remediation.

A central aspect of this study is the combination of commercially available photocatalytic filters with pre-existing metal-catalyst deodorising filters to achieve more practical solutions for VOC removal. By integrating these established technologies, we aim to enhance the practicality and effectiveness of VOC removal strategies. Furthermore, the use of commercially available photocatalytic filters alongside metal-catalyst deodorising filters represents progress towards more scalable solutions for VOC removal. This approach capitalises on the complementary strengths of both technologies, providing a robust

and versatile method for air purification. The findings of this research are expected to make a significant contribution to the development of advanced air purification systems, potentially enabling more efficient and sustainable approaches to managing indoor and outdoor air quality. Additionally, this study offers valuable insights into the complex interactions between various remediation technologies, forming a solid basis for future advancements in environmental catalysis and air purification systems. By deepening the understanding of these integrated processes, this research establishes a foundation for innovative applications and improvements in VOC removal.

2. Results and Discussion

2.1. The Morphologies of the Filters

Figure 1a illustrates the appearance of the metallic catalyst filter (left) and photocatalytic filter (right). Both filters measure 5 cm × 10 cm with a thickness of 1 cm. The surface microstructure of the photocatalytic filter was analysed using FE-SEM and EDX. Figure 1b presents the FE-SEM image, which reveals that the surface is densely covered with nanoparticles approximately several tens of nanometres in size. Figure 1c displays the results of SEM and EDX analysis. From left to right, the images show the SEM micrograph and elemental mapping of Ti, O, and Al atoms. These results indicate the presence of titanium dioxide nanoparticles on the surface of the alumina-based ceramic substrate.

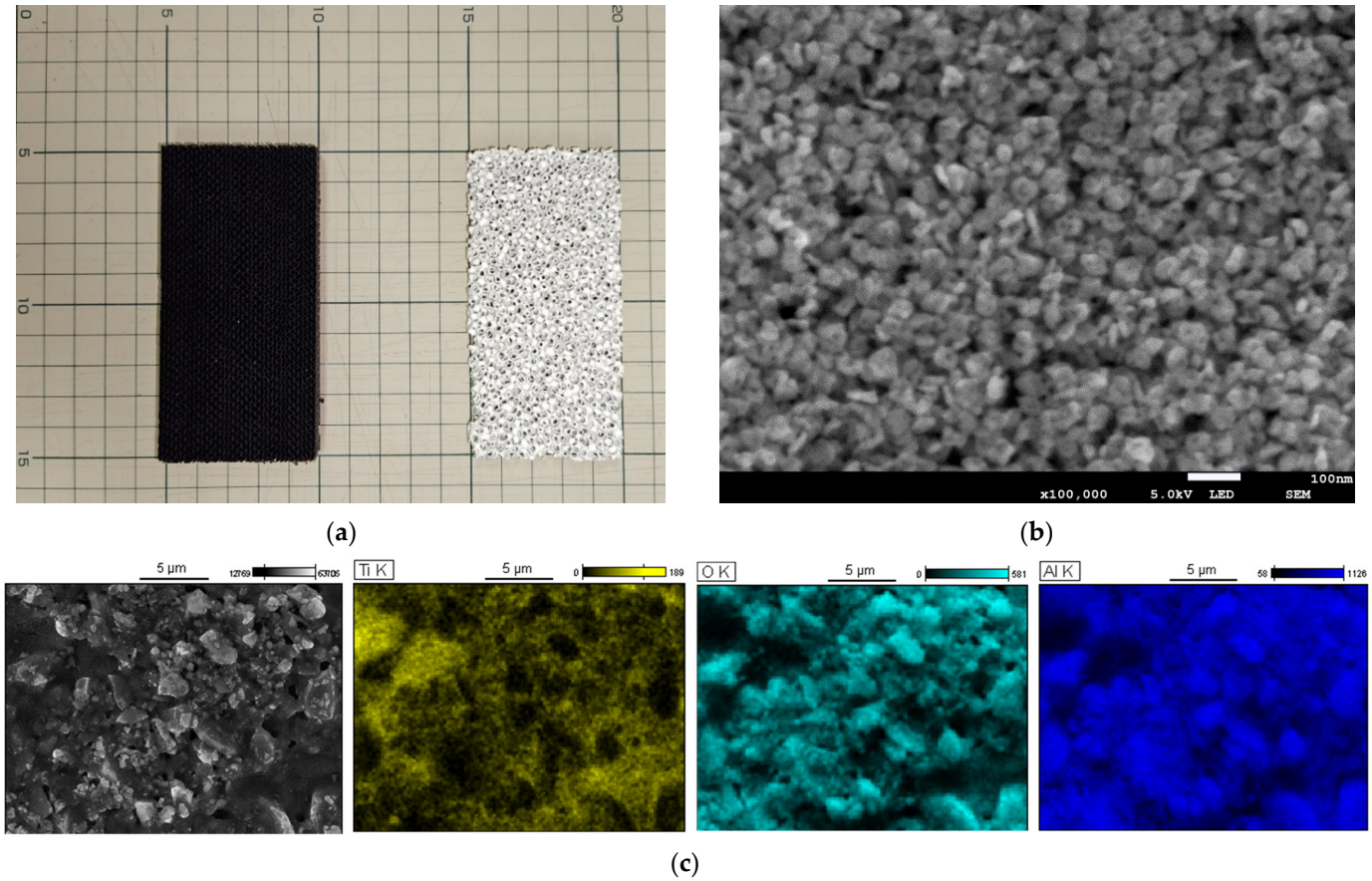

(**a**) (**b**)

(**c**)

Figure 1. Characterisation of the filters. (**a**) Photograph showing the metallic catalyst filter (**left**) and photocatalytic filter (**right**); (**b**) FE-SEM image of the photocatalytic filter surface showing uniform distribution of nanoparticles (scale bar: 100 nm); (**c**) SEM–EDX elemental mapping analysis of the photocatalytic filter surface showing the distribution of Ti, O, and Al atoms (scale bar: 5 µm).

2.2. Effect of Combining Metal-Catalyst Deodorising Filter, Photocatalytic Filter, and Ozone Gas Introduction

Figure 2a illustrates the concentration changes of acetaldehyde after passing through the existing deodorising filter. Although the filter effectively deodorised acetaldehyde initially, its performance declined over time, accompanied by minimal carbon dioxide production, suggesting limited decomposition of acetaldehyde. According to patent documentation, this filter adsorbs aldehydes effectively and regenerates its adsorption capacity by decomposing acetaldehyde when heated. In this study, however, the reaction was conducted at room temperature, resulting in adsorption effects only. The relatively high concentration of acetaldehyde likely caused the rapid saturation of the filter's adsorption capacity.

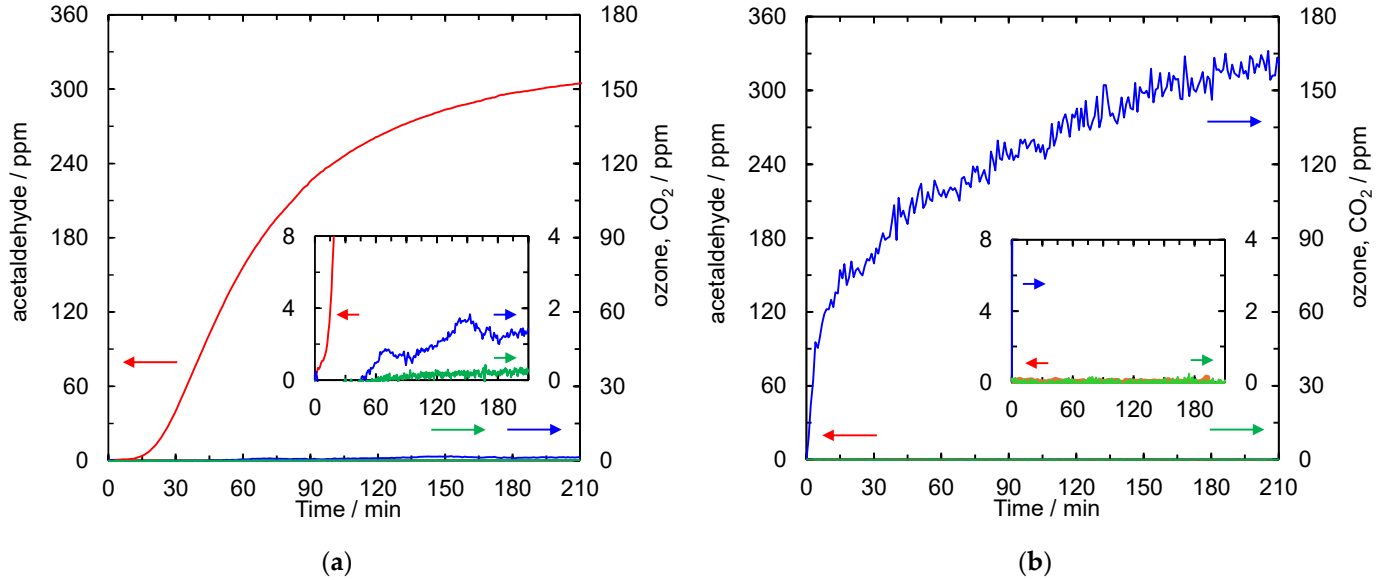

Figure 2. (**a**) Concentration changes of acetaldehyde when passed through the existing deodorising filter; (**b**) results of combining the photocatalytic filter and the existing deodorising filter with ozone gas introduction. Red: acetaldehyde; blue: CO_2; green: ozone. Inset: enlarged view of the vertical axis.

Figure 2b shows the results of combining the photocatalytic filter and the existing deodorising filter with ozone gas introduction. Even at the same acetaldehyde concentration, the outlet concentration did not increase. Furthermore, carbon dioxide, which was scarcely produced (Figure 2a), showed an increase over time. Similarly, the ozone concentration remained stable over an extended period. These observations suggest efficient acetaldehyde decomposition, which could not be achieved using the existing deodorising filter alone. Additional experiments were conducted by isolating each component to investigate the individual reactions and their contributions.

2.3. Effect of Combining Photocatalytic Filter and Ozone Gas Introduction

Building on the previous findings, the combined effect of a photocatalytic filter and ozone gas was further evaluated. Initially, acetaldehyde and ozone were introduced simultaneously. The individual contributions of the photocatalytic reaction, ozone oxidation, and their combined effect were examined in sequence. The supply concentrations of acetaldehyde and ozone, as well as the UV intensity, were kept consistent with those shown in Figure 1. The results are presented in Figure 3.

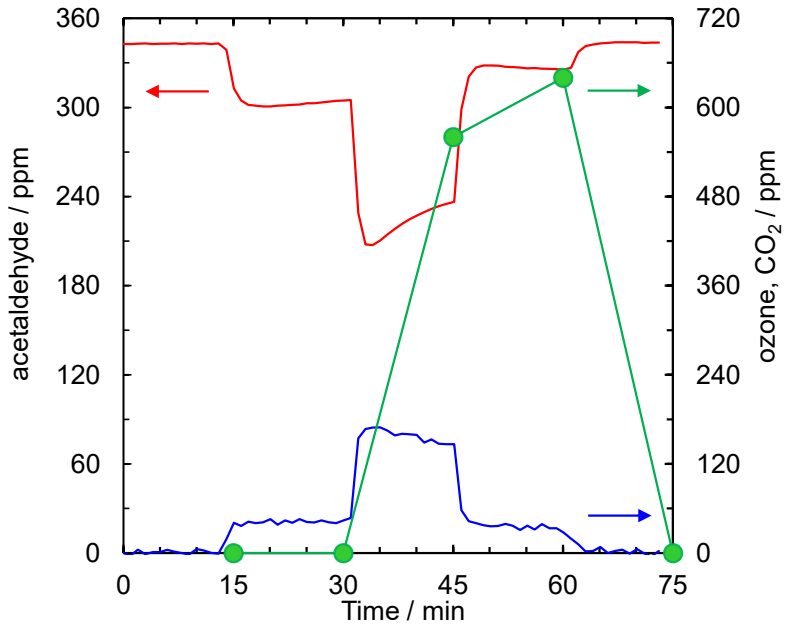

Figure 3. Effect of combining photocatalytic filter and ozone gas introduction. Red: acetaldehyde; blue: CO_2; green: ozone; 15 min: UV-C on; 30 min: ozone on; 45 min: UV-C off; 60 min: ozone off.

First, acetaldehyde gas was introduced into the photocatalytic filter until saturation adsorption was achieved, maintaining this state for 15 min (0–15 min). After 15 min, the UV lamps were switched on to initiate the photocatalytic reaction. This resulted in an immediate decrease in the acetaldehyde concentration and an increase in carbon dioxide concentration (15–30 min), indicating the decomposition of acetaldehyde into carbon dioxide via the photocatalytic process.

At the 30 min mark, ozone gas was introduced with the UV lamps still on. This further reduced the acetaldehyde concentration while increasing carbon dioxide concentration (30–45 min). Then, 15 min after ozone introduction, the outlet ozone concentration stabilised at approximately 80% of the supplied concentration (45 min, green dots). These findings suggest that the synergistic effect of the photocatalytic reaction and ozone oxidation enhanced acetaldehyde decomposition.

Between 45 and 60 min, the UV lamps were turned off while ozone gas continued to be introduced. The acetaldehyde concentration increased during this period, and the carbon dioxide concentration decreased. By the 60 min mark, the ozone concentration reached 90% of the supplied level (60 min, green dot), indicating that ozone oxidation alone contributed to acetaldehyde decomposition, although a significant portion of the ozone remained unreacted.

In a previous study, styrene was decomposed using photocatalysis and ozone in a similar manner [11]. While both previous and current studies have explored the synergistic potential of these processes, they have uncovered subtle differences in the decomposition pathways and efficiencies between acetaldehyde and styrene. For instance, fundamental structural distinctions between acetaldehyde (a simple aldehyde) and styrene (an aromatic compound) significantly influence their decomposition mechanisms.

In the current study, acetaldehyde exhibited a relatively straightforward decomposition pathway, primarily converting to acetic acid and subsequently to carbon dioxide. In contrast, earlier research on styrene identified a more complex transformation process, producing multiple intermediate products, including benzene, benzaldehyde, styrene oxide, and benzoic acid. This divergence underscores the critical role of molecular structure in determining the decomposition mechanisms during photocatalytic and ozone-assisted oxidation processes.

The aromatic ring in styrene introduces additional complexity compared with the linear structure of acetaldehyde, resulting in a more intricate decomposition pathway. Both our studies demonstrated enhanced decomposition efficiency when photocatalysis and ozone treatment were combined. In the current study, the integration of photocatalysis and ozone gas resulted in greater acetaldehyde decomposition than photocatalysis alone. Similarly, previous research found that the combined treatment was more effective than either method independently, achieving approximately 70% removal of styrene with minimal production of toxic intermediates. A key insight from both studies is the importance of monitoring intermediate products. Previous research has particularly highlighted the potential toxicity of intermediates such as benzene and styrene oxide, both of which are carcinogenic. This emphasises the necessity of conducting a comprehensive analysis that extends beyond removal efficiency to assess the safety and environmental impact of the intermediate by-products.

An interesting divergence has emerged concerning the role of UV irradiation. In a previous study, UV light (primarily in the 310–380 nm range) did not significantly accelerate decomposition. The light above 310 nm was found to be insufficient for effectively generating excited singlet oxygen and hydroxyl radicals. Considering this, the acetaldehyde study employed UV-C irradiation (5 mW/cm^2 at 254 nm), which appeared to play a more active role in facilitating photocatalytic decomposition. Conversely, Huang et al. utilised vacuum ultraviolet (VUV) irradiation for photocatalytic benzene decomposition [16]. A key breakthrough in their research was the significant increase in benzene removal efficiency when combining photocatalysis with VUV irradiation, which promoted ozone formation. The superior performance of the catalyst in their study was attributed to its optimised porous structure and framework, which enhanced benzene adsorption and ozone degradation capabilities, as discussed in the subsequent section.

These differences are likely due to variations in the experimental setup, catalyst composition, and the specific molecular characteristics of the target compounds. These comparative findings underscore the complexity of photocatalytic and ozone-assisted VOC decomposition. Factors such as molecular structure, experimental conditions, and catalyst composition significantly influence the decomposition pathway and efficiency.

2.4. Effect of Combining a Deodorising Filter with a Metal Catalyst and Ozone Gas Introduction

The effects of combining a deodorising filter containing a metal catalyst with ozone gas were investigated. Based on the findings from previous sections, a fixed amount of acetaldehyde was first introduced into the deodorising filter using a metal catalyst to facilitate adsorption. After halting the supply of acetaldehyde, ozone gas was introduced, and the resulting changes in the concentrations of various gases were monitored.

The supply ratios of acetaldehyde and ozone were adjusted across four stages, ranging from 0.1 to 9.3. The results for one stage, with a ratio of 5, are shown in Figure 4. Initially, 70 ppm of acetaldehyde gas was introduced at a flow rate of 1 L/min into the deodorising filter containing a metal catalyst for 60 min (0–60 min). The acetaldehyde concentration at the reactor outlet began rising immediately, eventually exceeding 80% of the supply concentration by the end of the 60 min period. At the 60 min mark, the acetaldehyde supply was halted, and 700 ppm of ozone gas was introduced at the same flow rate for 30 min. The acetaldehyde concentration initially exhibited a temporary increase before decreasing rapidly. Concurrently, the carbon dioxide concentration temporarily rose and then gradually declined (60–90 min).

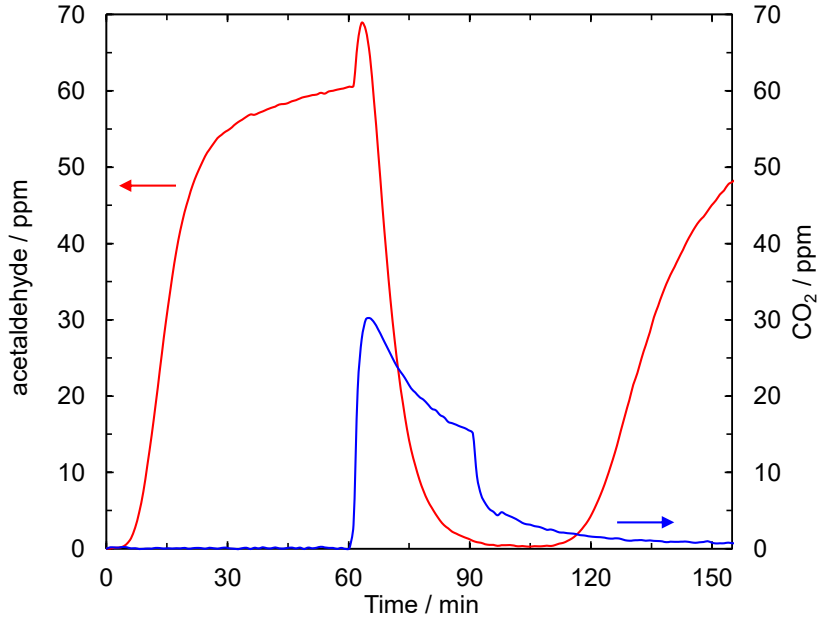

Figure 4. Effect of combining a deodorising filter with a metal catalyst and ozone gas introduction. Red: acetaldehyde; blue: CO_2; 60 min: acetaldehyde off, ozone on; 90 min: ozone off, air on; 95 min: acetaldehyde on.

After stopping the ozone gas supply, synthetic air was introduced at the same flow rate for 5 min to purge any residual ozone gas (90–95 min). Subsequently, 70 ppm of acetaldehyde gas was reintroduced for 60 min. During this second introduction, the acetaldehyde concentration increased at a slower rate compared to the initial introduction (95–155 min). Furthermore, the ozone concentration at the reactor outlet did not increase during the 60–90 min period, indicating that all introduced ozone was decomposed by the metal catalyst and effectively utilised for acetaldehyde decomposition.

Our investigation revealed a significant enhancement in acetaldehyde removal efficiency following ozone exposure, attributed to the interaction between ozone and the metal-catalyst surface. This phenomenon may be linked to ozone decomposition on the catalyst surface, resulting in the formation and retention of highly oxidative O_2^{2-} species [17].

Interactions between ozone and metal-oxide catalysts, particularly manganese-based systems, are well-documented. Previous studies have shown that catalyst deactivation during ozone decomposition often results from the accumulation of O_2^{2-} species on the catalyst surface. Comprehensive research by Li et al., involving long-term activity testing, X-ray photoelectron spectroscopy (XPS), and density functional theory (DFT) calculations, identified two types of oxygen vacancies in manganese dioxide catalysts. One type exhibited a greater tendency for oxygen species adsorption, leading to catalyst deactivation [18].

In advancing catalyst regeneration, Liao et al. proposed a liquid-phase method to remove O_2^{2-} species from oxygen vacancies using a reducing solution with an oxidation–reduction potential below −163 mV [17]. Their experiments demonstrated that, even after 10 deactivation–regeneration cycles, surface oxygen vacancies and metal valence states could be effectively restored, with ozone conversion rates maintaining stability within 5% of the initial values. However, our study offers a distinct perspective on the role of retained O_2^{2-} species. Unlike previous research, which primarily focused on their deactivating effects, our findings suggest that these species actively enhance VOC removal efficiency. Retained O_2^{2-} species were observed to react rapidly with incoming acetaldehyde molecules, increasing removal rates. This discovery challenges the traditional view of O_2^{2-} accumulation as solely detrimental to catalyst performance. Instead, it

highlights a more complex mechanism in which these species act as active intermediates in VOC oxidation.

The implications extend beyond acetaldehyde removal, offering potential strategies for designing advanced catalytic systems. These systems could leverage the oxidative power of retained O_2^{2-} species while mitigating their deactivating effects. This research opens new directions for exploring the optimal balance between ozone exposure, O_2^{2-} formation, and VOC removal efficiency, paving the way for more effective and sustainable VOC removal technologies.

The supply ratios of acetaldehyde and ozone; the cumulative removal amount of acetaldehyde; the amount of decomposition products, such as carbon dioxide; and the calculated and measured TOC values are summarised in Table 1.

Table 1. Summary of acetaldehyde and ozone supply ratios, cumulative acetaldehyde removal, decomposition product distribution, and calculated and measured TOC values.

Supply Ratios of Acetaldehyde/Ozone	**0.1**	**1**	**5**	**9.3**
cumulative removal amount of acetaldehyde (μmol)	1813	2406	960	579
desorption amount of acetaldehyde (μmol)	529	640	156	46
adsorption amount of acetaldehyde (μmol)	952	838	133	31
converted to acetic acid (μmol)	19	816	566	350
converted to CO_2 (μmol)	17	116	79	78
calculated TOC value (mg/L)	233	397	168	91
measured TOC value (mg/L)	261	306	173	106

As presented in Table 1, with one stage and an acetaldehyde/ozone ratio of 5, approximately 60% of the removed acetaldehyde was converted into acetic acid. Of the remaining 40%, 30% was either adsorbed onto or desorbed from the filter as acetaldehyde, while the final 10% was predominantly converted to carbon dioxide. Other potential decomposition products of acetaldehyde, such as formic acid and formaldehyde, were below the detection limit under the test conditions. The total organic carbon (TOC) measurements aligned with the values calculated from the adsorbed acetaldehyde and acetic acid amounts, confirming that formic acid and formaldehyde were scarcely produced.

Similar tests were conducted under the other three conditions, and the results are summarised in Table 1 and Figure 5. As the ozone supply increased relative to acetaldehyde, the proportion of acetaldehyde converted to acetic acid also increased. However, this conversion plateaued between supply ratios of 5.0 and 9.3. The proportion converted to carbon dioxide showed a slight increase from 5.0 to 9.3. These findings suggest that, in the presence of the metal catalyst and ozone, the decomposition of acetaldehyde tends to halt at the acetic acid stage rather than progressing fully to carbon dioxide.

A review by Liu et al. [14] provided in-depth insight into the complex interactions between metal catalysts and ozone in removing volatile organic compounds (VOC). This analysis serves as a robust reference for discussing the acetaldehyde degradation observed in this study. A key highlight of the review is the versatility of catalytic ozonation as a low-temperature VOC removal strategy. Unlike traditional high-temperature oxidation methods, catalytic ozonation is both energy-efficient and environmentally sustainable. This study focuses on two primary reaction mechanisms—Langmuir–Hinshelwood and Mars–van Krevelen—detailing how different metal catalysts interact with ozone and organic compounds. It also emphasises that catalytic performance is strongly dependent on the specific VOC being treated. Among the catalysts studied, manganese oxide-based materials have consistently emerged as the most active for catalytic ozonation. This aligns with the findings of previous research on metal catalysts. The metal catalyst used in this study was

also manganese oxide-based, reaffirming its status as an optimal choice for low-temperature VOC decomposition.

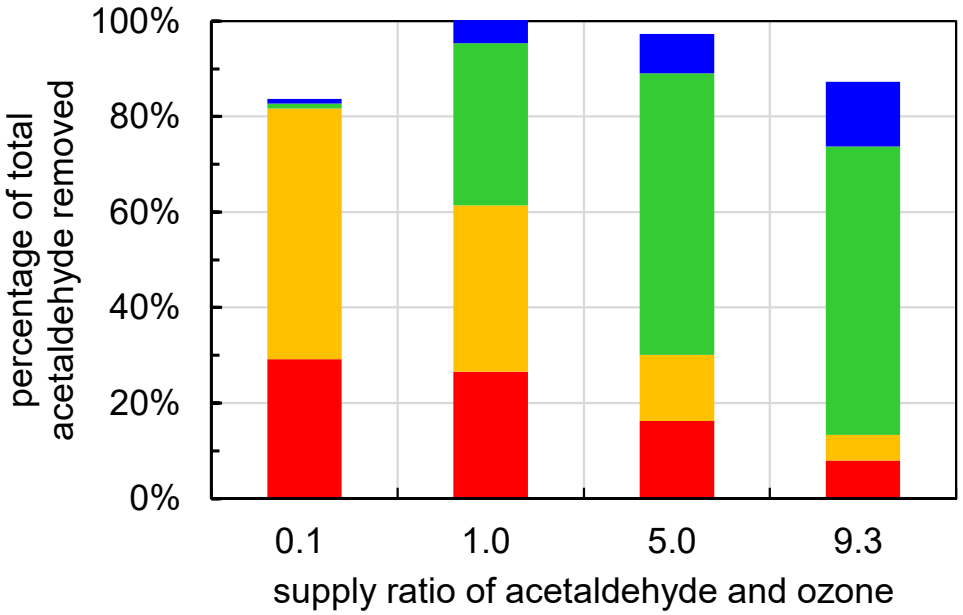

Figure 5. Effect of combining a deodorising filter using a metal catalyst with ozone gas introduction. Red: desorption amount of acetaldehyde; orange: adsorption amount of acetaldehyde; green: converted to acetic acid; blue: converted to CO_2.

2.5. Estimated Degradation Pathways of Photocatalyst Filter + Ozone and Metal-Catalyst Filter + Ozone

The decomposition mechanisms of acetaldehyde under different catalytic conditions reveal complex interactions between photocatalytic and metal-catalysed oxidation processes. Drawing upon the work of Muggli et al. [19] on ethanol decomposition using isotope labelling, we traced the reaction pathways of acetaldehyde, which acts as an intermediate in ethanol oxidation. Their research provided valuable insights into the subsequent transformation mechanisms of acetaldehyde, offering a foundation for understanding its direct decomposition processes in our study.

Based on the findings presented in previous sections, we analysed the decomposition mechanisms and identified potential rate-determining steps under each experimental condition. These mechanisms are summarised in Figure 6, highlighting the distinct pathways and interactions in the presence of the photocatalyst filter and ozone compared with the metal-catalyst filter and ozone.

In the photocatalyst filter + ozone system, observations revealed the rapid conversion of acetaldehyde beyond acetic acid, with minimal acetic acid detected. This indicates that the rate-determining step likely occurs before acetic acid formation, enabling subsequent decomposition to proceed efficiently. The photocatalytic process likely generates highly reactive hydroxyl radicals through the interaction of UV light with TiO_2, while ozone contributes additional oxidative species. This synergy accelerates the complete mineralisation of acetaldehyde into CO_2 and H_2O.

In contrast, the metal-catalyst filter + ozone system exhibited distinct characteristics, with acetic acid emerging as the stable intermediate. This suggests that the rate-determining step occurs after acetic acid formation, thereby limiting further decomposition. The mechanism likely involves ozone decomposition on the metal-catalyst surface, generating active oxygen species that facilitate the initial oxidation of acetaldehyde but lack sufficient oxidative potential for complete mineralisation.

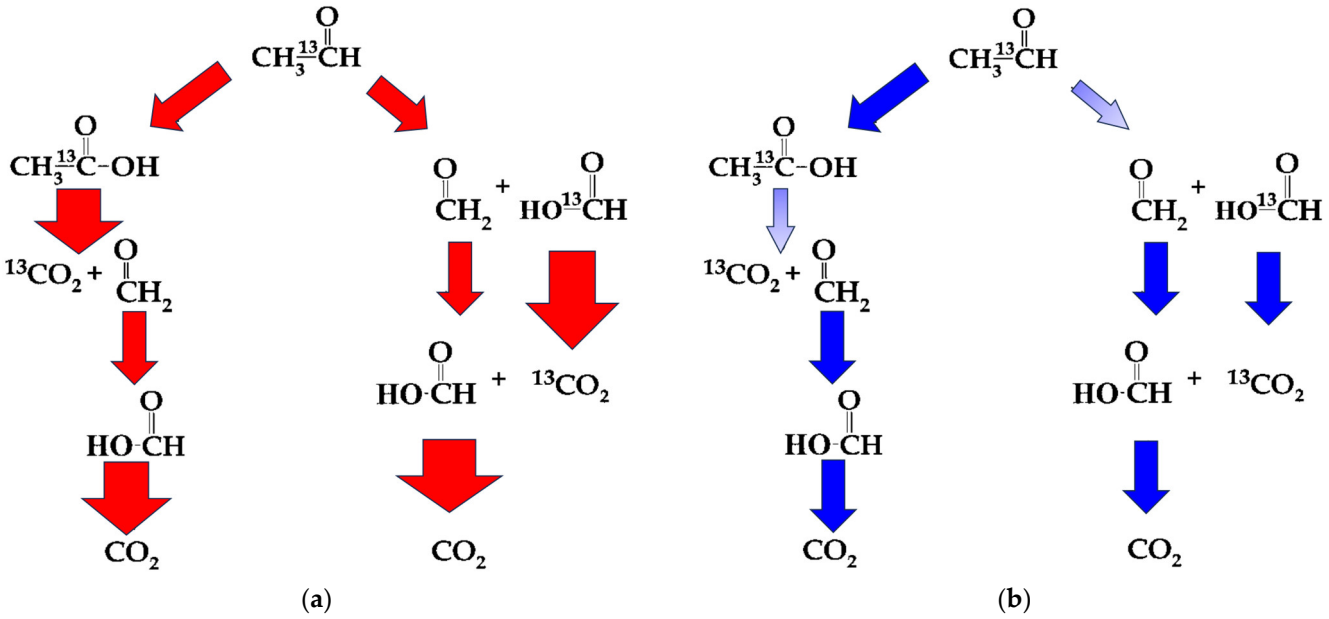

Figure 6. Estimated degradation pathways. (**a**) Photocatalyst filter + ozone (red arrow); (**b**) metal-catalyst filter + ozone (blue arrow). The rate-determining step is indicated by a light–colored arrow. Reproduced with permission from Muggli, D.S. et al., Journal of Catalysis 1998, 173, 470–483 [19].

These mechanistic differences align with insights from Liu et al. [14], who comprehensively reviewed catalytic ozonation processes. Their analysis identified two primary mechanisms: Langmuir–Hinshelwood, where both ozone and VOCs adsorb onto the catalyst surface before reacting, and Mars–van Krevelen, which involves the participation of lattice oxygen. Our metal-catalyst system likely operates through a combination of these mechanisms, with the dominant pathway dependent on the specific reaction conditions.

The remarkable synergy observed when both filters were combined (Figure 2b) can be attributed to the complementary nature of their rate-determining steps. Photocatalytic systems efficiently manage later-stage decomposition, while metal-catalyst systems excel in the initial oxidation phase. This mechanistic complementarity creates a more robust oxidation system capable of complete mineralisation. The studies by Huang et al. [20] and Yuan et al. [21] provide a thorough exploration of VOC decomposition mechanisms using integrated photocatalytic and oxidation processes. Their research on TiO_2/M-ZSM-5 catalysts (where M = Zn, Cu, or Mn) systematically evaluated the effects of transition-metal ion exchange on acetaldehyde decomposition. Notably, manganese-exchanged catalysts demonstrated superior decomposition efficiencies under UV–ozone conditions, underscoring the potential of strategically incorporating metal ions into catalytic systems.

This study explores the synergistic interactions between photocatalysis, ozone treatment, and metal catalysts in the decomposition of acetaldehyde, a representative volatile organic compound (VOC). The study addresses the growing need for efficient air purification technologies by integrating advanced oxidation processes. This approach builds upon comprehensive research by El Khawaja et al., who emphasised that VOCs pose significant health and environmental risks, particularly in mixtures or during repeated exposures, even at trace levels. Their review highlighted that coupling different VOC treatment techniques can create more efficient systems while reducing energy consumption [22].

Metal catalysts, particularly manganese oxide-based materials, were combined with photocatalysis and ozonation to investigate their impact on acetaldehyde removal efficiency. This strategy was inspired by the groundbreaking work of Nie et al., who demonstrated exceptional VOC removal efficiency using Pd/TiO_2@carbon nanofibrous microspheres. Their research achieved remarkable conversion rates of 96.4% and 91.7% for toluene and

benzene, respectively, highlighting the crucial synergistic effects between metal catalysts and TiO_2 in photocatalytic processes [23].

Experimental results revealed that the treatment integrating these methods significantly outperformed conventional single-process treatments. This finding aligns with research by Ding et al., who demonstrated that ternary heterojuncted nanocomposites with 3D ordered macroporous (3DOM) structure can significantly enhance photocatalytic performance through improved light harvesting, abundant reactive sites, and efficient charge separation. Their work with platinum/bismuth molybdate/3DOM TiO_2 composites showed that optimised heterojunction structures can dramatically improve both photocatalytic and thermal catalytic performance in VOC decomposition [24].

Metal catalysts facilitated the initial oxidation of acetaldehyde, while photocatalysis accelerated subsequent stages, including the mineralisation of intermediates. The importance of catalyst stability and complete mineralisation was further emphasised by Hou et al., who demonstrated that porous β-Ga_2O_3 photocatalysts could achieve benzene conversion rates approximately 10 times higher than conventional TiO_2 (P25), with remarkable stability over 80 h of continuous operation. Their findings on the relationship between specific surface area, oxidative capability, and long-term stability provided valuable insights for our catalyst design [25].

Ozone contributed additional reactive oxidative species, further enhancing decomposition rates. This multi-component approach addresses the challenges identified by El Khawaja et al. regarding the complexity of VOC mixtures and the need for efficient, energy-conscious treatment methods. The successful integration of multiple treatment approaches in our study demonstrates the potential for developing more effective air purification technologies, building upon the materials innovation demonstrated by both Nie et al. and Ding et al., while maintaining the operational stability highlighted by Hou et al.

This approach has significant potential applications in environmental remediation and indoor air quality management. By combining the insights from these previous studies on catalyst design, heterojunction engineering, and process integration, our work contributes to the ongoing development of more efficient and sustainable air purification technologies.

A consistent theme across these studies and the current investigation is the emphasis on the synergistic interactions between different oxidation processes. Rather than treating adsorption, ozonation, and photocatalytic reactions as isolated mechanisms, their interconnected dynamics warrant deeper investigation. These studies highlight the importance of understanding how different catalytic components interact to enhance overall pollutant decomposition efficiency.

3. Materials and Methods

3.1. Materials and Analytical Methods

All materials used in this study were commercially sourced. The photocatalytic filter was obtained from S·E·E Co., Ltd. (Yokohama, Japan), while the metal-catalyst filter was developed using the technology described in Patent WO2010007978A1 [26]. Each sample was shaped into dimensions of 5 × 10 × 1 cm and installed in a photocatalytic test reactor for the Acetaldehyde Removal Test, following JIS R1701-2 [27] and ISO 22197-2 [28] standards, with an adapter specifically designed for filter testing.

Changes in the concentration of test gases were analysed using a photoacoustic multigas analyser, Gasera ONE (Gasera Ltd., Turku, Finland), equipped with filters for acetaldehyde, acetic acid, and carbon dioxide. Additional analyses were conducted using gas chromatography–mass spectrometry (GC–MS) with a GCMS-QP2010SE system (Shimadzu, Kyoto, Japan), fitted with a capillary column (TC-BOND-Q, 30 m length × 0.25 mm inner diameter × 0.8 μm film thickness, Agilent Technologies, Santa Clara, CA, USA). The

GC–MS analysis involved an initial oven temperature of 30 °C, which was held for 3 min, followed by a temperature increase to 200 °C over 6 min at a rate of 40 °C/min, with a split ratio of 10.9.

In addition, the test gases and decomposition products adsorbed onto the filter after testing were analysed by washing the filter with pure water, and the wash solution was subsequently examined using GC–MS. Ion chromatography was performed to identify decomposition products retained on the filter, using a Tosoh Corporation IC-2001 ion chromatograph with a TSK-GEL SuperIC-AZ column maintained at 40 °C. The eluent consisted of an aqueous solution of 7.5 mmol/L $NaHCO_3$ and 1.1 mmol/L Na_2CO_3, delivered at a flow rate of 0.8 mL/min.

TOC analysis was conducted with a TOC analyser (TOC-L CPH with OCT-L; Shimadzu Co., Kyoto, Japan) using the TC-IC method.

The morphologies of the photocatalyst filter were observed using a Schottky Field Emission Scanning Electron Microscope (FE-SEM, JSM-7800F Prime; JEOL Ltd., Tokyo, Japan). The acceleration voltage was 5 kV. Energy-dispersive X-ray spectroscopy (EDS) was performed using the NORAN System7 (Thermo Fisher Scientific, Waltham, MA, USA). The measurement was conducted with an acceleration voltage of 15 kV.

3.2. VOC Decomposition Test

An example of the test conditions is illustrated in Figure 7, which corresponds to the data presented in Figure 1b. The upper section of Figure 7 shows the state of the sample removed from the reactor alongside the adapter used for filter testing. The metal catalyst and photocatalytic filters were stacked and installed within the JIS reactor. As indicated by the arrows, the test gas entered from the lower right of the figure, flowed upward through the filter section, passed first through the metal-catalyst filter, then through the photocatalytic filter, and exited from the upper left.

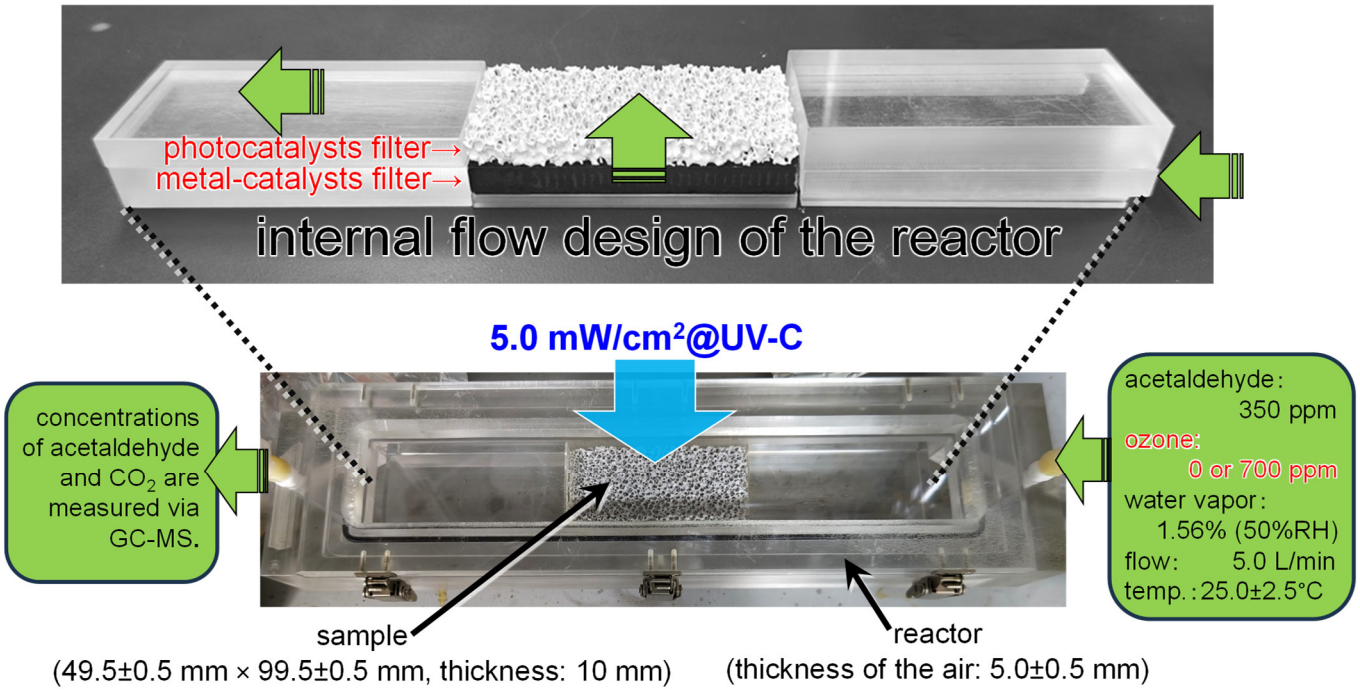

Figure 7. An example of the test conditions. Green arrow: gas; Blue arrow: UV light.

The test gas flow rate was set to 1.0 L/min, the temperature was maintained at 25 ± 2 °C, and the relative humidity was controlled at 50 ± 10%. Initially, synthetic air was passed through the system for 1 h to remove any pre-adsorbed substances. Subsequently,

acetaldehyde was mixed with synthetic air to a concentration of 350 ppm, along with ozone at 700 ppm. Simultaneously, a germicidal lamp irradiated the sample through a quartz window (UV-C, 5 mW/cm^2 at 254 nm). Changes in the concentrations of acetaldehyde, ozone, and carbon dioxide at the reactor outlet were monitored using a photoacoustic multigas analyser.

The filters were then washed with pure water, and the resulting wash solution was analysed using GC–MS and ion chromatography to determine the amounts of substances adsorbed onto the filters. TOC analysis was also performed. Variations in the sequence of filter placement, as well as the type, concentration, and flow rate of the test gases, were examined to assess their effects on the decomposition process.

4. Conclusions

The integration of multiple processes produced a synergistic effect, enabling efficient decomposition. The design and optimisation of the reaction system are essential for developing practical air purification systems. The following future research directions are proposed based on these findings:

- Further investigation of the effects of transition metal ions on catalytic performance;
- Exploration of catalyst stability and long-term effectiveness;
- Expansion of research to include a broader range of volatile organic compounds;
- Development of a more comprehensive understanding of the degradation pathways.

While previous studies have explored various combinations of these technologies using powder mixtures or supported catalysts, this study presents the first successful demonstration of integrating commercially available metal catalysts and photocatalysts on filter substrates with ozone treatment for enhanced VOC decomposition. This practical approach offers immediate potential for real-world applications while maintaining high decomposition efficiency. This study systematically explores advanced oxidation processes for VOC decomposition. It contributes to the ongoing development of more effective environmental remediation technologies by evaluating various approaches to catalyst design and process integration.

Author Contributions: Conceptualisation, methodology, data curation, writing—original draft, T.O.; investigation, validation, T.O., K.H., and M.O.; writing—review and editing, M.O. All authors have read and agreed to the published version of the manuscript.

Funding: This study received no external funding.

Data Availability Statement: Data are contained within the article.

Acknowledgments: We would like to thank Ryo Takahashi and Daisuke Aoki (KISTEC) for analysing the reaction products. We also would like to thank Misa Nishino (KISTEC) for observing the morphologies of the photocatalyst filter.

Conflicts of Interest: Author Michifumi Okui was employed by the company Fuji Industrial, Co., Ltd. The remaining authors declare that the research was conducted in the absence of any commercial or financial relationships that could be construed as a potential conflict of interest.

Abbreviations

The following abbreviations are used in this manuscript:

DFT	Density functional theory
TOC	Total organic carbon
VUV	Vacuum ultraviolet
VOCs	Volatile organic compounds
XPS	X-ray photoelectron spectroscopy

References

1. Fujishima, A.; Honda, K. Electrochemical photolysis of water at a semiconductor electrode. *Nature* **1972**, *238*, 37–38. [CrossRef] [PubMed]
2. Fujishima, A.; Zhang, X.; Tryk, D.A. TiO_2 photocatalysis and related surface phenomena. *Surf. Sci. Rep.* **2008**, *63*, 515–582. [CrossRef]
3. Ochiai, T.; Fujishima, A. Photoelectrochemical properties of TiO_2 photocatalyst and its applications for environmental purification. *J. Photochem. Photobiol. C* **2012**, *13*, 247–262. [CrossRef]
4. Hou, W.-M.; Ku, Y. Photocatalytic decomposition of gaseous isopropanol in a tubular optical fiber reactor under periodic UV-LED illumination. *J. Mol. Cat. A Chem.* **2013**, *374–375*, 7–11. [CrossRef]
5. Huang, Y.; Ho, S.S.H.; Lu, Y.; Niu, R.; Xu, L.; Cao, J.; Lee, S. Removal of indoor volatile organic compounds via photocatalytic oxidation: A short review and prospect. *Molecules* **2016**, *21*, 56. [CrossRef]
6. Benoit-Marquié, F.; Wilkenhöner, U.; Simon, V.; Braun, A.M.; Oliveros, E.; Maurette, M.-T. VOC photodegradation at the gas–solid interface of a TiO_2 photocatalyst: Part I: 1-butanol and 1-butylamine. *J. Photochem. Photobiol. A* **2000**, *132*, 225–232. [CrossRef]
7. Ochiai, T.; Aoki, D.; Saito, H.; Akutsu, Y.; Nagata, M. Analysis of adsorption and decomposition of odour and tar components in tobacco smoke on non-woven fabric-supported photocatalysts. *Catalysts* **2020**, *10*, 304. [CrossRef]
8. Gervasini, A.; Vezzoli, G.C.; Ragaini, V. VOC removal by synergic effect of combustion catalyst and ozone. *Catal. Today* **1996**, *29*, 449–455. [CrossRef]
9. Zhang, P.; Liu, J. Photocatalytic degradation of trace hexane in the gas phase with and without ozone addition: Kinetic study. *J. Photochem. Photobiol. A* **2004**, *167*, 87–94. [CrossRef]
10. Huang, H.; Li, W. Destruction of toluene by ozone-enhanced photocatalysis: Performance and mechanism. *Appl. Catal. B Environ.* **2011**, *102*, 449–453. [CrossRef]
11. Hamada, K.; Ochiai, T.; Aoki, D.; Akutsu, Y.; Hirabayashi, Y. Decomposition of gaseous styrene using photocatalyst and ozone treatment. *Catalysts* **2022**, *12*, 316. [CrossRef]
12. Kim, H.-S.; Kim, H.-J.; Kim, J.-H.; Kim, J.-H.; Kang, S.-H.; Ryu, J.-H.; Park, N.-K.; Yun, D.-S.; Bae, J.-W. Noble-metal-based catalytic oxidation technology trends for volatile organic compound (VOC) removal. *Catalysts* **2022**, *12*, 63. [CrossRef]
13. Comparelli, R. Special issue: Application of photoactive nanomaterials in degradation of pollutants. *Materials* **2019**, *12*, 2459. [CrossRef]
14. Liu, B.; Ji, J.; Zhang, B.; Huang, W.; Gan, Y.; Leung, D.Y.C.; Huang, H. Catalytic ozonation of VOCs at low temperature: A comprehensive review. *J. Hazard. Mater.* **2022**, *422*, 126847. [CrossRef]
15. Ma, G.; Guan, J.; Zhu, Q.; Jiang, Y.; Han, N.; Chen, Y. A review of ozone decomposition by a copper-based catalyst. *Catalysts* **2024**, *14*, 264. [CrossRef]
16. Huang, H.; Liu, G.; Zhan, Y.; Xu, Y.; Lu, H.; Huang, H.; Feng, Q.; Wu, M. Photocatalytic oxidation of gaseous benzene under VUV irradiation over TiO_2/zeolites catalysts. *Catal. Today* **2017**, *281*, 649–655. [CrossRef]
17. Liao, J.; Cheng, H.; Fang, Y.; Zhang, Y.; Zhao, X.; Qiu, L.; Cai, X.; Zhang, X. Regeneration of ozone decomposition catalysts by elimination of O_2^{2-} from oxygen vacancies. *J. Environ. Chem. Eng.* **2024**, *12*, 113573. [CrossRef]
18. Li, X.; Ma, J.; Zhang, C.; Zhang, R.; He, H. Detrimental role of residual surface acid ions on ozone decomposition over Ce-modified γ-MnO_2 under humid conditions. *J. Environ. Sci.* **2020**, *91*, 43–53. [CrossRef]
19. Muggli, D.S.; McCue, J.T.; Falconer, J.L. Mechanism of the photocatalytic oxidation of ethanol on TiO_2. *J. Catal.* **1998**, *173*, 470–483. [CrossRef]
20. Huang, X.; Yuan, J.; Shi, J.; Shangguan, W. Ozone-assisted photocatalytic oxidation of gaseous acetaldehyde on TiO_2/H-ZSM-5 catalysts. *J. Hazard. Mater.* **2009**, *171*, 827–832. [CrossRef]
21. Yuan, J.; Huang, X.; Chen, M.; Shi, J.; Shangguan, W. Ozone-assisted photocatalytic degradation of gaseous acetaldehyde on TiO_2/M-ZSM-5 (M=Zn, Cu, Mn). *Catal. Today* **2013**, *201*, 182–188. [CrossRef]
22. El Khawaja, R.; Veerapandian, S.K.P.; Bitar, R.; Geyter, N.D.; Morent, R.; Heymans, N.; Weireld, G.D.; Barakat, T.; Ding, Y.; Abdallah, G.; et al. Boosting VOCs elimination by coupling different techniques. *Chem. Synth.* **2022**, *2*, 13. [CrossRef]
23. Nie, L.; Duan, B.; Lu, A.; Zhang, L. Pd/TiO_2 @ Carbon Microspheres Derived from Chitin for Highly Efficient Photocatalytic Degradation of Volatile Organic Compounds. *ACS Sustain. Chem. Eng.* **2019**, *7*, 1658–1666. [CrossRef]
24. Ding, Y.; Huang, L.; Barakat, T.; Su, B.-L. A Novel 3DOM TiO_2 Based Multifunctional Photocatalytic and Catalytic Platform for Energy Regeneration and Pollutants Degradation. *Adv. Mater. Interfaces* **2021**, *8*, 2001879. [CrossRef]
25. Hou, Y.; Wang, X.; Wu, L.; Ding, Z.; Fu, X. Efficient Decomposition of Benzene over a β-Ga_2O_3 Photocatalyst under Ambient Conditions. *Environ. Sci. Technol.* **2006**, *40*, 5799–5803. [CrossRef]
26. Nariyuki, A.; Hashimoto, S.; Aikawa, R.; Takeuchi, K.; Tozuka, Y. Deodorizing Catalyst, Deodorizing Method using Same and Method for Regenerating the Catalyst. Japan WO2010007978A1, 21 January 2010.

27. *JIS R 1701-2: 2016*; Fine Ceramics (Advanced Ceramics, Advanced Technical Ceramics)—Test Method for Air Purification Performance of Photocatalytic Materials—Part 2: Removal of Acetaldehyde. Japanese Standards Association: Tokyo, Japan, 2016.
28. *ISO 22197-2: 2019*; Fine Ceramics (Advanced Ceramics, Advanced Technical Ceramics)—Test Method for Air-Purification Performance of Semiconducting Photocatalytic Materials—Part 2: Removal of Acetaldehyde. International Organization for Standardization: Geneva, Switzerland, 2019.